

## Groundwater flow and transport modeling of MTBE at Rocky Mount, Virginia, USA

Syed Mobasher Aftab<sup>1\*</sup> and Warren T Dean<sup>2</sup>

<sup>1</sup>Balochistan University of IT, Engineering & Management Sciences, Quetta

<sup>2</sup>ATS International, Inc. Christiansburg, VA, USA

\*Corresponding author's email: syed.mobasher@buitms.edu.pk

Submitted date: 12/10/2019 Accepted date: 15/02/2020 Published online: 30/03/2020

### Abstract

Groundwater flow and transport modeling conducted for court litigation at Plateau Plaza, Rocky Mount, VA, USA. In October 1999 about 6,500 to 7,500 liters of petroleum released to the subsurface. Many residential and commercial water supply wells impacted by dissolved phase MTBE. The study objective is to evaluate travel time of dissolved phase MTBE from site to individual properties of supply wells, MS-7 and MS-9. Groundwater flow and dissolved phase transport models were constructed using MODFLOW and MT3D. The two-layered model was conceptualized and constructed using historical drilling data, groundwater gauging, sampling, slug-testing, and geophysical studies. Flow and transport models calibrated to historical groundwater levels and concentrations. Sensitivity analysis conducted to evaluate uncertainty in hydraulic conductivity, dispersivity, and source concentration. The conclusions based on geologic, hydrogeologic, geophysical and dissolved concentration data spanning over eight years that portray actual field conditions. The specific dates of dissolved MTBE movement and to approach the boundaries of individual properties based on modeling and professional expertise. The model is sensitive to change in any parameter that would affect the plume speed. Any changes to those parameters, including changes that would slow the migration of the simulated plume were detrimental to the calibration of the model. It is appraised that the dissolved MTBE entered the property of Well No. MS-7 in the deep and upper zones in December 31, 2001, and February 24, 2002, respectively. The plume in the property of Well No. MS-9 entered in deeper and upper zones in September 11, 2002, and October 13, 2002.

*Keywords:* Flow model, Transport model, MTBE, Litigation.

### 1. Introduction

The StopIn-Plateau Plaza (Plateau Plaza) facility consists of a retail fuel station, and other small businesses at the intersection of US Highway 220 and Wirtz Road, at Rocky Mount, Virginia (Fig. 1). Numerous individual residential and commercial water supply wells exist in the vicinity of the Plateau Plaza site, some of which have been impacted by dissolved phase methyl tertiary butyl ether (MTBE). The objective of this study is to evaluate the time of travel of dissolved phase MTBE from the petroleum release location at the Plateau Plaza to some individual properties. The supply wells (SW) at individual properties are identified in Figure 2 as SW-7, and the supply well SW-9. The study was conducted to; construct and calibrate a groundwater flow computer model; to utilize the flow field from the groundwater model to calibrate a contaminant transport model of dissolved

phase MTBE, and to simulate the calibrated transport model to evaluate the travel time from the release to the properties of Well Nos. SW-7 and SW-9.

The modeling effort builds on a previous modeling study by ATS in 2004 (ATS International, 2004). The current modeling study considers a larger study area than the previous study and incorporates additional data obtained since 2004. The additional data include lithologic data from drilling, monitoring well-gauging data from new and previously existing wells, and dissolved phase MTBE data from sampling events between 2004 and 2007. The 2004 studies included information on regional fracture systems, information on local fracture systems interpreted from a resistivity imaging geophysical study, and regional groundwater gradients based on monitoring well-gauging data and local surface streams.

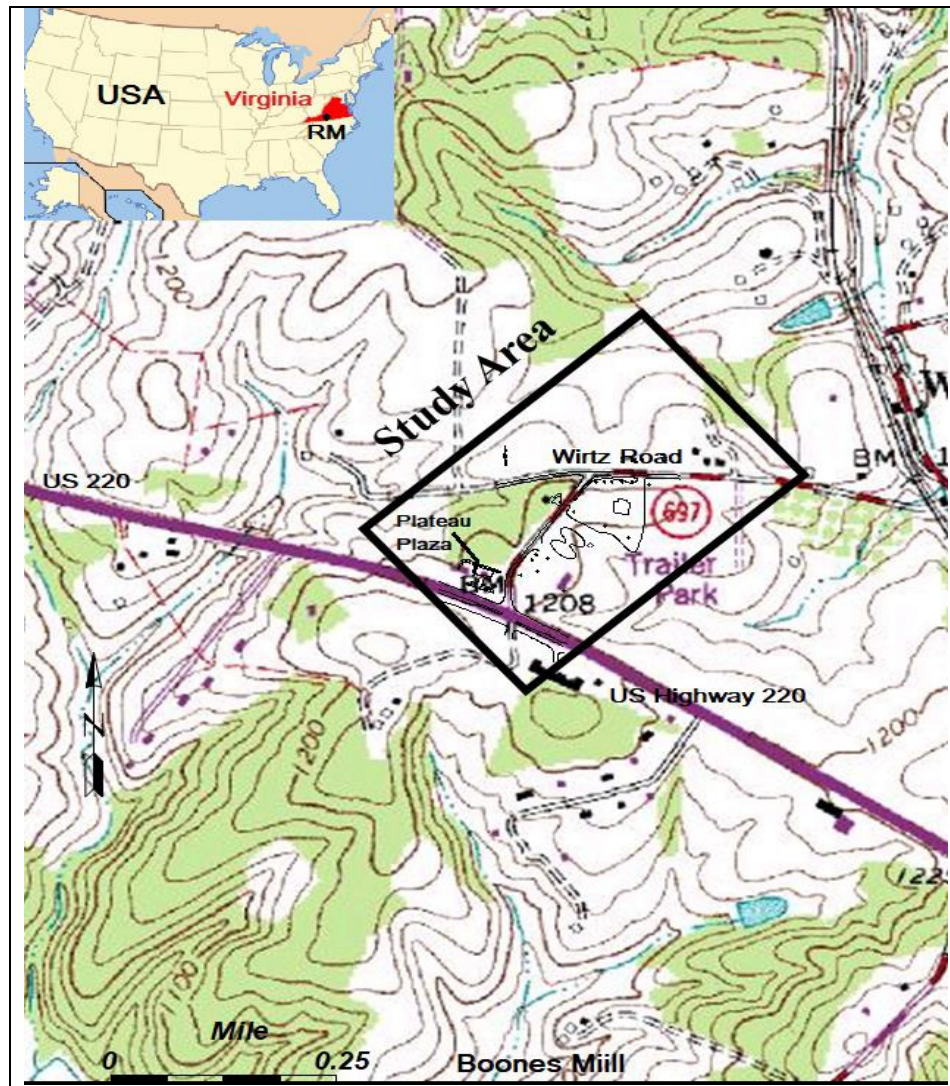


Fig. 1. Location map and topography of study area, Boones Mill 7½-minute USGS topographic quadrangle, Rocky Mount, Virginia, USA.

### 1.1. Site history

October 13, 1999, the site experienced a petroleum release from a leaking fuel line where an estimated 6,500 to 7,500 liters of gasoline were lost to the subsurface near dispensers 3 and 4 (IMS, 2000). A site characterization report (SCR) was requested by the Virginia Department of Environmental Quality (DEQ), which was submitted by IMS Environmental Services, Inc. (IMS) in January 2000. The SCR included the results of the installation, gauging, and sampling of three monitoring wells, and the advancement, and sampling of four soil test borings, along with a sampling of the station's potable water well. The DEQ review of the SCR and request for quarterly monitoring reports submitted in July 2000 by IMS. The report included the results of

sampling of three additional soil borings, conversion into monitoring wells, gauging, and sampling of all six monitoring wells. The second Post SCR submitted in February 2003 included the results of gauging and sampling of the six existing monitoring and eight private potable water supply wells near the site (Apex Environmental, 2003). The SCR Addendum No. 2 was submitted in July 2003 (Crawford Environmental Services, 2003). This report included the results of the advancement along-with sampling of four additional soil borings off-site, conversion into monitoring wells, gauging, and sampling of all wells. The aquifer characterization estimated through slug tests of two on-site monitoring wells, contaminant modeling of benzene and MTBE using BIOSCREEN.

The SCR Addendum No. 3 was submitted in January 2004 (Crawford Environmental Services, 2004a). This report included the results of sampling of six additional soil borings off-site, conversion into monitoring wells. Gauging and sampling of all off-site and on-site wells, and sampling of one spring near the site. The SCR Addendum No. 4 was submitted in May 2004 (Crawford Environmental Services, 2004b). This report included the results of the advancement and sampling of additional five off-site and seven on-site soil borings. Conversion of six borings into monitoring wells, gauging, and sampling of all twenty-two monitoring wells. The sampling of two private potable water supply wells near the site, sampling of an unnamed pond near the site, contaminant modeling of benzene and MTBE using BIOSCREEN, and a 120-hour dual-phase extraction at monitoring well number 6 (MW-6). The SCR Addendum

No. 5 was submitted in September 2004 (Crawford Environmental Services, 2004c). The report comprised sampling results of nineteen on and off-site monitoring wells, sampling of ten private potable water supply wells, and a 120-hour dual-phase extraction at monitoring well MW-6. The SCR Addendum No. 6 was submitted in April 2005 (ECS, 2005). This report summarized all work to date for the site characterization phase. Geophysical information and the results of a dual-phase extraction pilot test were included in SCR Addendum No. 7 (ECS, 2006a). The deep zone monitoring well installation, gauging, and sampling was documented in SCR Addendum No. 7 (ECS, 2006b). A Corrective Action Plan was submitted in 2007 (ECS, 2007). This report contains a comprehensive compilation of all groundwater levels and concentration data on which current modeling effort is based.

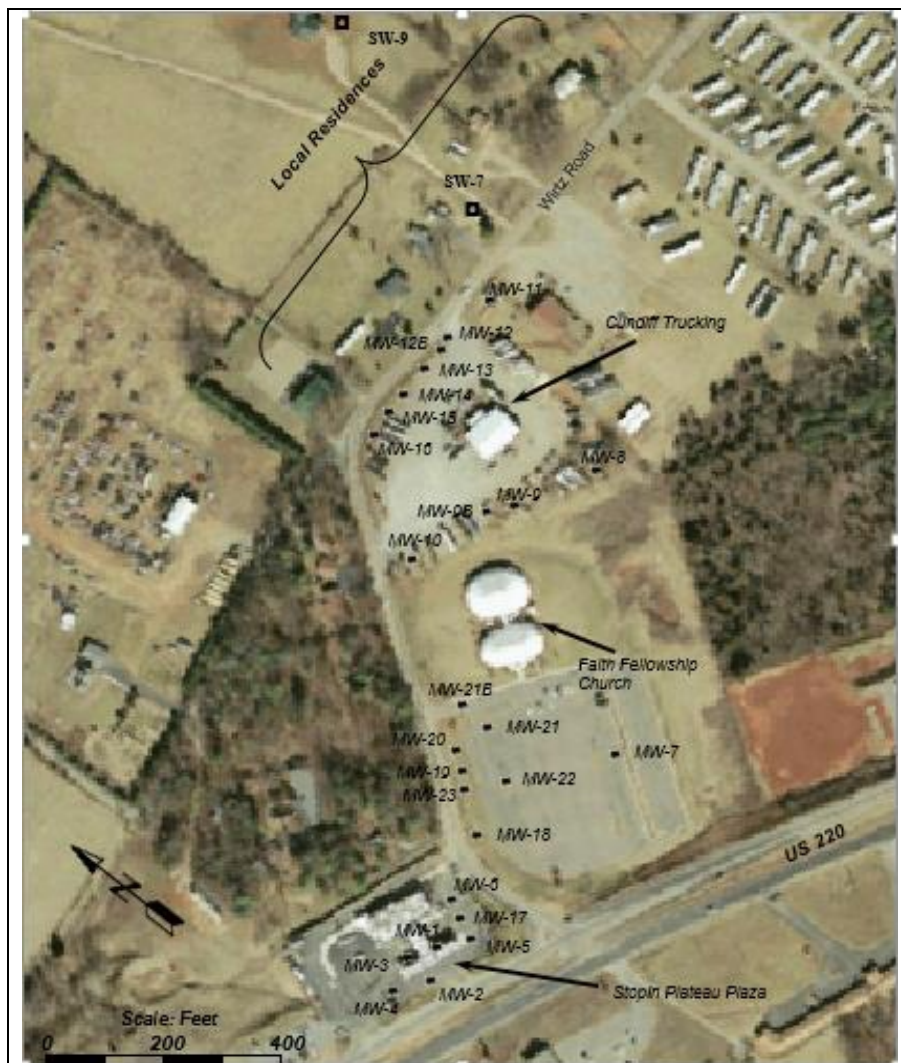


Fig. 2. Site plan illustrating major features and locations of monitoring wells.

## 2. Local geology

The site is located in the Rocky Mount to Boones Mill Corridor in the northwestern margin of the Piedmont Province and is underlain by what has been described by Henika (2004) as meta-igneous and meta-sedimentary rocks of the Ashe and Alligator Back formations. In both the Ashe and Alligator Back Formations, local schistosity and foliations trend universally to the northeast between 30 and 60 degrees (Fig. 3). Drilling data from the site indicate that the local lithology is comprised of an intermediate meta-volcanic sequence comprised of metamorphosed ash and volcanoclastic. Local schistosity in both the Ashe and Alligator Back Formations is evidence of ancient tectonism. Data from the drilling and coring from the site suggest that what has been mapped as the contact between the Alligator Back and Ashe formations is representative of a fracture zone trending to the northeast (Fig. 4).

The structural analysis of the study area was performed by using aerial photographs and shaded relief maps. The shaded relief maps were constructed from a digital elevation model (DEM) data. Fracture traces represent the surface expression of subsurface fractures or fault zones. They expressed on aerial photographs and shaded relief maps as straight stream segments or valleys, aligned surface depressions, gaps in ridges, or other features displaying a linear orientation. The interpreted fracture traces were mapped and the shaded relief map and their orientations measured and recorded. The most prominent fracture orientation trends to the northwest with a lesser set trending northeast (Fig. 5).

Among geophysical studies, an electrical resistivity survey was conducted. Electrical resistivity surveying techniques are used to determine the thickness and resistivity of underground geological formations for estimating groundwater potential. Electrical resistivity surveys conducted to acquire an exhaustive subsurface structure to identifying the fracture systems that impact groundwater flow into shallow deeper aquifer zones. Resistivity lines 1 and 2 reveal a relatively horizontal soil zone overlying fractured

bedrock in the site area (Fig. 6). Line 1 has a thin horizontal layer of low resistivity material near the surface underlain by a very high resistivity zone containing vertically oriented low resistivity areas. The black dashed line illustrates the top of bedrock. The high resistivity in the bedrock represents the massive biotite gneiss described by Henika (2004). The low resistivity in the bedrock is vertically oriented fracture zones that extend upward into the shallow unconsolidated layer. The vertical fractures are due to Late Paleozoic-Mesozoic compressive tectonic forces. This type of thrust-faulted structure occurs throughout the Blue Ridge and Piedmont provinces. The high resistivity in the lower part of the soil interval represents weathered bedrock (saprolite) and the shallow horizontally oriented low resistivity zone is the semi-saturated soil interval. Line 2 indicating the presence of different types of bedrock and unconsolidated materials on the eastern portion of the site. The bedrock zone has low to intermediate resistivity revealing the presence of vertical fracture zones (low resistivity) and foliated metamorphic rock. Line 2 shows considerable variation in the resistivity above the top of bedrock. High variability in the resistivity distribution above bedrock reflects the different types of unconsolidated materials due to weathering of the bedrock and the degree of water saturation in that interval.

## 3. Hydrogeology of study area

The hydrogeologic investigations provide information about aquifer geometry, boundary conditions, and aquifer properties. The structural pattern, lithological logs, groundwater level monitoring, aquifer testing, geochemical analysis, and geophysical studies provide additional information regarding aquifer geometry and flow regime. The local hydrogeology of the site area is quite complex. The exposed geological formations, structural pattern and topographical relief complicate the groundwater flow system. To study the groundwater flow and spread of contamination plume 26 monitoring wells were installed in the area. The monitoring wells cover a major part of the area along the downgradient of flow direction towards the northeast of the site. The location plan of monitoring wells is shown in

Figure 2. The monitoring wells were installed from a period of 1999 to 2007, most of the wells drilled during 2003 and 2004, and ranging in depth from 58 to 75 ft. Four deep monitoring wells were drilled, two in 2006 and two in 2007 with a depth ranging from 85 to 154 ft. The

lengths of well screens vary from 10 to 40 ft, and the bedrock encountered at a depth of 40 to 60 ft below ground level (fbgl). The monitoring well drilling dates and relevant data is presented in Table 1.

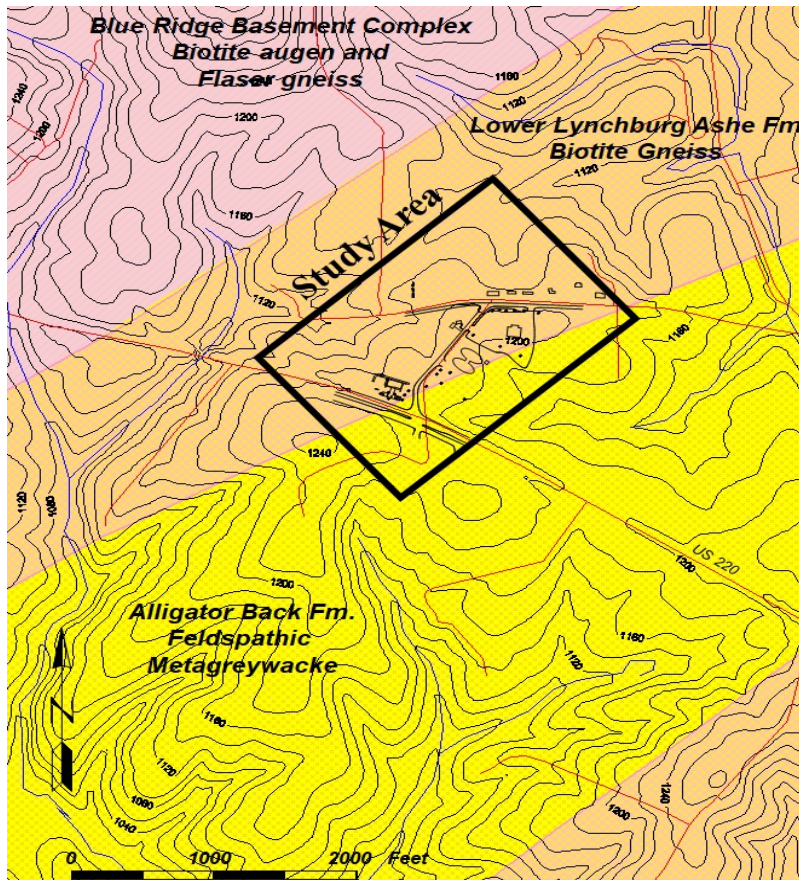


Fig. 3. Generalized geologic map of the site and surrounding area, (Henika, 2004).

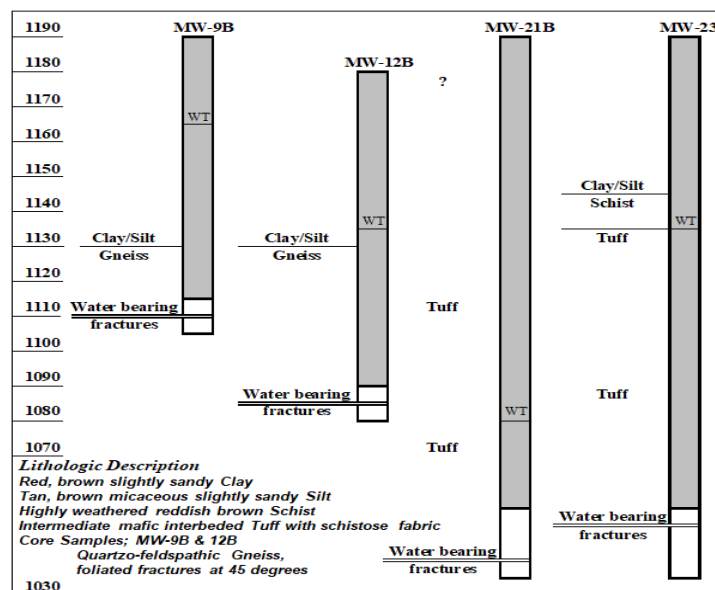


Fig. 4. Deep Monitoring Well Designs, showing the subsurface lithology and location of water-bearing fractures.

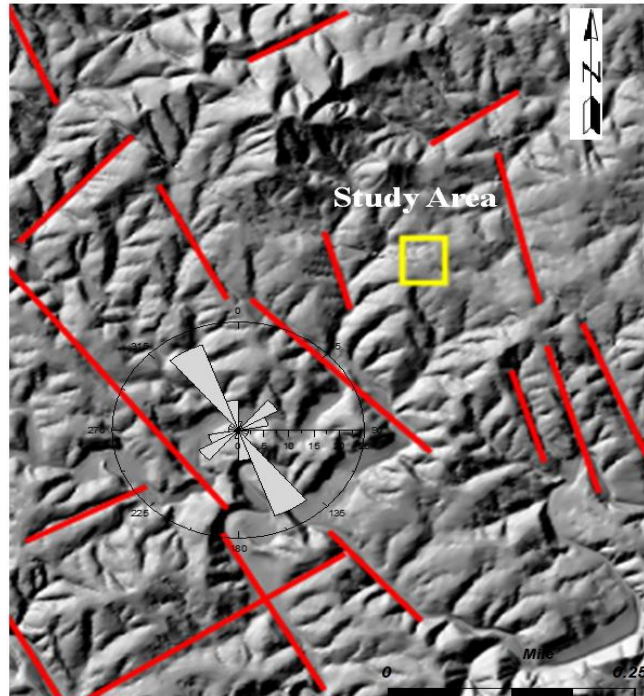


Fig. 5. Shaded relief map and Rose Diagram of site and surrounding area illustrating fracture trace analysis.

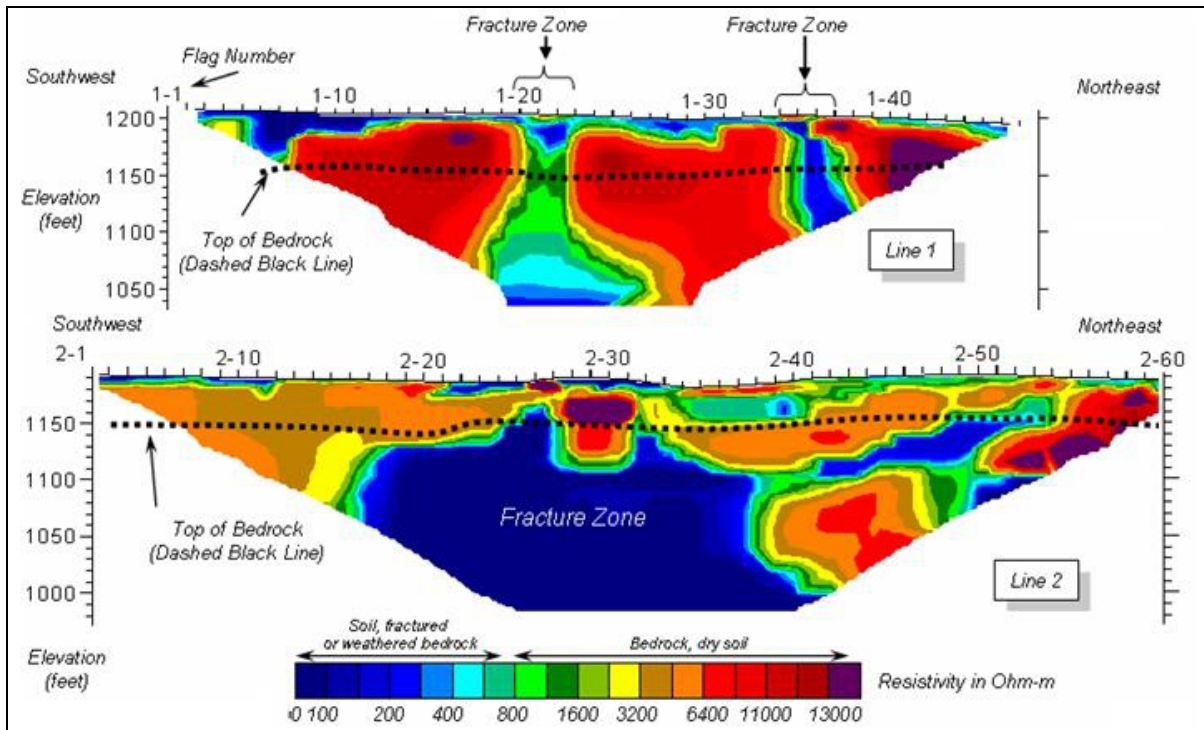


Fig. 6. Resistivity sections for lines 1 and 2 collected over the site, fracture zones interpreted at top of bedrock.

Table 1. Monitoring wells construction data along-with average and standard deviation of well monitoring data.

Well ID	Installation Date	Well Depth (ft)	Screen Depth (ft)	Screen Length (ft)	Bedrock Depth (ft)	Well Monitoring	
						Average (ft MSL)	Standard Deviation
MW-1	4-Nov-99	65	40	25	45	1145	1.8
MW-2	4-Nov-99	62	37	25	40	1146	0.7
MW-3	4-Nov-99	85	45	40	45	1147	0.9
MW-4	16-May-00	72	42	30	50	1151	7.2
MW-5	16-May-00	70	40	30	60	1146	0.9
MW-6	16-May-00	73	43	30	50	1149	11.3
MW-7	16-Jun-03	60	40	20	52	1142	1.8
MW-8	16-Jun-03	60	40	20	53.8	1141	1.6
MW-9	16-Jun-03	60	40	20	51.3	1136	0.8
MW-9B	22-Jun-06	85	75	10	58	1134	2.2
MW-10	16-Jun-03	60	40	20	48	1137	1.2
MW-11	9-Dec-03	75	35	40	45	1131	1.7
MW-12	8-Dec-03	75	35	40	60	1132	2.3
MW-12B	22-Jun-06	100	90	10	52	1134	0.6
MW-13	8-Dec-03	75	35	40	48	1135	0.7
MW-14	8-Dec-03	75	35	40	53	1145	10.7
MW-15	8-Dec-03	75	35	40	48	1141	5.1
MW-16	9-Dec-03	75	35	40	40	1139	2.2
MW-17	22-Mar-04	60.5	30.5	30	48	1151	14.8
MW-18	22-Mar-04	58.3	29	30	55	1145	0.9
MW-19	22-Mar-04	60.5	30.5	30	45	1145	1
MW-20	22-Mar-04	59.2	30	30	48	1146	1.4
MW-21	22-Mar-04	60	30	30	54	1141	1.6
MW-21B	29-Mar-07	154	134	20	52	1078	30.8
MW-22	22-Mar-04	60.5	30.5	30	53	1141	0.7
MW-23	29-Mar-07	154	134	20	53	1137	0

The local soils affected by geology, landforms, climate, relief, and natural vegetation. The soils are formed of materials weathered from basement rocks which are mica rich in nature. The site area is underlain by 40 to 60 ft thick layer of soil and clay. The clay represents a wide range of colors from reddish to brownish and grayish. The fine-grained, sandy to silty at places, the loamy clay is micaceous in composition (lithological logs of MW-6, 17 and 23). The clay layer is overlain by a thick sequence of meta-igneous and meta-sedimentary rocks composed of schist, gneiss, and tuff. The schist is grey, reddish and brown, (lithological logs of MW-6 and 23). The intermediate mafic interbedded tuff with schistose fabric encountered at MW-21B and 23. The quartzo-feldspathic gneiss mostly foliated and fractured observed at MW-9B,

lithology represents by three core samples taken from 62 to 72 ft depths. The lithological composition at MW-12B represents quartzo-feldspathic gneiss with a quartz/feldspar intrusion at 65 ft, two core samples were taken from 58.5 to 68.5 fbg. The lithological logs of deep monitoring wells MW-9B, 12B, 21B and 23 represent the presence of major water-bearing fractures at depths ranging from 80 to 140 fbg. The presence of large fractures at greater depths increased the hydraulic conductivity and relevant hydraulic properties at depths along with secondary porosity and permeability. In general, the primary porosity in hard rocks is much smaller than secondary porosity. The groundwater flows rapidly through hard rock along with secondary porosity, the secondary porosity represents fracture including faults, joints, bedding planes

and contact zones of different lithological units, which have much larger effective porosity. The fracture size, orientation, and their interconnectivity control the flow and hydraulic conductivity of groundwater at certain depths and levels. The lithological logs and the position of large water-bearing fractures of some monitoring wells are presented in Figure 4.

### 3.1. Groundwater monitoring

Monitoring well-gauging data is available from 1999 to 2007. Hydrographs of the water levels indicate that most of the wells display little fluctuation over time, (Fig. 7 (a, b)). The degree of water level fluctuation is quantified by the standard deviation. Twenty of the 26 wells display a standard deviation of fewer than 2.5 feet, indicating a low degree of fluctuation (Table 1). The standard deviation of five wells, including MW-4, MW-6, MW-14, MW-17, and MW-21B, that ranges from 7.2 to 30.8 feet.

High water level fluctuations can sometimes be attributed to changes in the groundwater flow direction, changes in gradient, the influence of variable recharge, and potentially by pumping of nearby water supply wells. However, examining the data it reveals that for most of the wells displaying high standard deviation, it is the result of one or more anomalous values. To ensure that the modeling effort included only high-quality data, those wells displaying a standard deviation of greater than 5 feet were not included in the model. The low degree of water level fluctuation in the wells indicates that the average of the water level data is representative of the historical water table characteristics. Therefore, the flow direction and gradient remain relatively constant with time. A contour map of the average water levels is provided in Figure 8. Using this contour map, the average groundwater gradient at the site is 0.016 ft/ft flowing to the northeast. A localized groundwater trough is observed in the central portion of the study area.

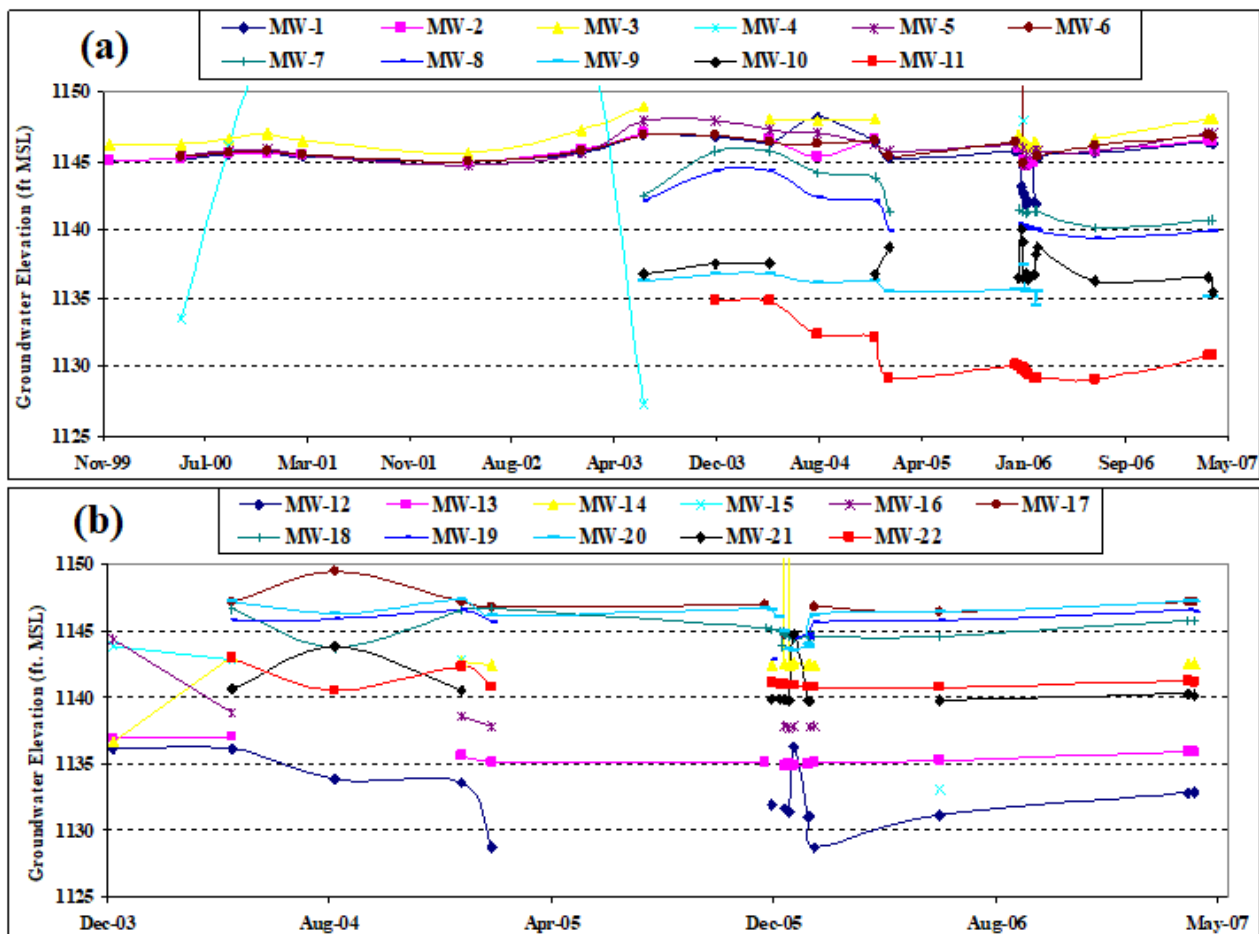


Fig. 7. Time vs. Groundwater Elevation Graphs of Monitoring Wells.  
a). Monitoring Wells MW 1-11. b). Monitoring Wells MW 12-22.

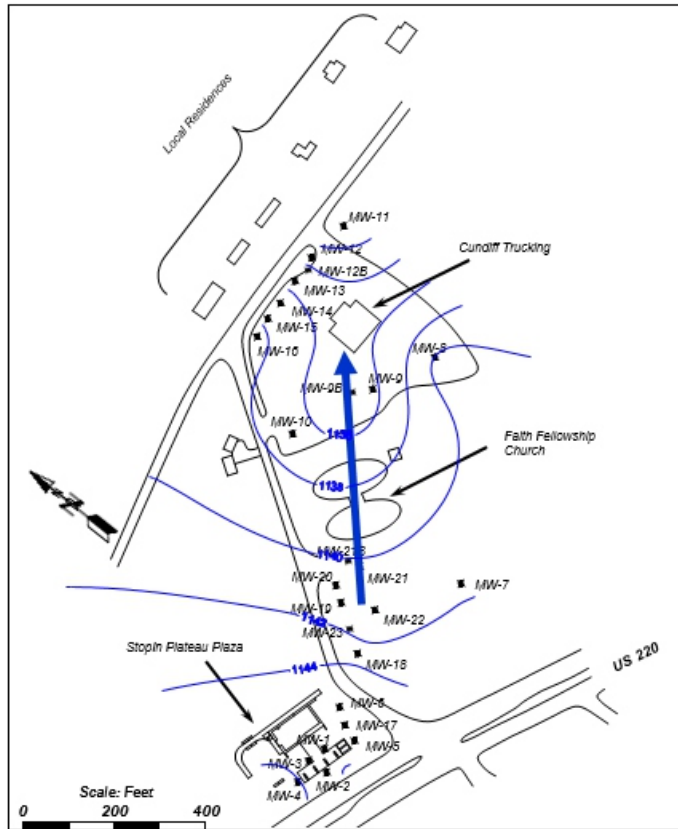


Fig. 8. Groundwater Table Map of the area, contours drawn with average values of 17 monitoring wells.

#### 4. Conceptual geologic model

The geophysical data were integrated with the topographic, geologic, hydrogeologic, structural, and borehole information to create a conceptual geologic model of the site (Fig. 9). The conceptual model serves as the basis for the construction of the numerical computer model. Work by Henika (2004) suggests that the site is bisected by the contact between biotite gneiss of the Ashe Formation and feldspathic metagraywacke of the Alligator Back Formation (Fig. 3). More recent drilling data tends to contradict Henika's interpretation of the lithology. However, all of the geologic and hydrogeologic data are consistent with the presence of a narrow, highly transmissive zone that trends from southwest to northeast. The drilling, slug test, and the gauging data are consistent with the presence of a well-developed fracture zone along with the contact between the Ashe and Alligator Back Formations. The trend of this fracture zone is consistent with the regional strike of the bedrock towards the northeast. The orientation of the cleavage and foliation in the bedrock and the overlying saprolite is also toward the

northeast. This pattern in the subsurface causes a preferred groundwater flow direction along with that trend and can be a conduit for high groundwater flow (Fleck and White, 1989; Harned and Daniel, 1989). The site data suggests the presence of two water-bearing zones, one in the upper portion of the aquifer and one in the deep zone. However, because of the high degree of hydraulic communication between the two zones and the absence of an appreciable amount of data about the degree of interconnection between the two zones, the two water-bearing zones were simulated in this modeling effort as one aquifer.

#### 5. Groundwater flow modeling

The groundwater modeling files were created and run using the modeling interface Visual MODFLOW version 4.2 (Waterloo Hydrogeologic, 2006). Visual MODFLOW uses a graphical interface to create and run the finite difference numerical model created by McDonald and Harbaugh of the US Geological Survey in 1988. MODFLOW is a three-dimensional finite-difference groundwater flow model that simulates steady-state and

transient flow in an irregularly shaped flow system in which aquifer layers can be confined, unconfined or a combination of both. Based on the conceptual geologic model and the relatively uniform groundwater flow direction and gradient, the flow was simulated as steady-state flow occurring in unconfined to the semi-confined aquifer of uniform thickness. The model domain has dimensions of 2000 x 1500 x 120 feet, covering an area of about 0.108 square miles. The model was constructed of a finite difference grid, comprised of 80 rows and 60 columns with a maximum grid spacing of 25 x 25 feet in both the X and Y directions. The grid mesh was refined into 12.5 x 12.5 feet in the central part of the model which comprises monitoring wells. The mesh size at the hydrocarbon release site refined into 6.25 x 6.25 ft to precisely allocate the source area to simulate the temporal variations in contaminant flux arising from water table fluctuations at the source. The model is comprised of three vertical layers, every 40 feet in thickness. The uppermost soil and saprolite zone, while the second and third layers represent the basement rock with different hydraulic conductivities as upper zone and deeper zones of the aquifer. The aquifer is simulated as shallow unconfined to semi-confined conditions occurring near the soil-bedrock interface.

Constant head boundaries were defined around the perimeter of the model domain to simulate boundaries at which water levels remain constant throughout the simulation. The constant head boundary condition is used to fix the head value in selected grid cells, thus acting as an infinite source of water entering or leaving the system. The average water table contours of the aquifer were mapped and overlaid on the model grid, and the constant heads around the model domain were extrapolated from the contoured water table. The site receives an average of 44 inches of precipitation per year. A considerable amount of precipitation infiltrates to the groundwater system as surface recharge. To simulate vertical recharge to the aquifer through precipitation, each cell in the top layer of the model domain was assigned a recharge rate. The recharge zones in the model were defined ranging from 0 to 0.006 ft/day. The covered areas such as roads and parking lots receive no vertical recharge. Grass covered

areas and forests lose significant amounts of precipitation due to evapotranspiration and runoff. Drainage ditches receive runoff from other areas and have high values for vertical recharge. The various recharge zones defined in the model are illustrated in Figure 10. The recharge rates used in the flow model in feet per day are also presented in the same figure.

### 5.1. Flow parameters

Slug tests and pump tests were conducted to estimate the site-specific hydraulic conductivity (K) values. The estimated hydraulic conductivity values of five wells vary from 0.04 to 2.6 ft/day. The estimated transmissivity values of the same wells vary from 0.4 to 26.2 ft<sup>2</sup>/day. The estimates of K from the slug and pump tests analysis are presented in Table 2, (Crawford Environmental Services, Inc., 2003; ECS Mid-Atlantic, LLC, 2007). Six K zones were defined in the groundwater flow model (Table 3). The geometry and K value of each zone was guided by the conceptual geologic model for the site (Fig. 11). Each K zone has a different value for longitudinal hydraulic conductivity (K<sub>x</sub>), transverse hydraulic conductivity (K<sub>y</sub>), and vertical hydraulic conductivity (K<sub>z</sub>), reflecting the anisotropy of bedrock aquifer. The northeast-trending strike of the bedrock and the northwest-trending fractures provide the geologic basis for the placement of elongated high K zones in the computer model. Based on borehole logging data, the bedrock aquifer can be separated into two vertical components or zones. The upper zone is characterized by lower conductivities as compared to the deeper zone that contains discrete water-bearing fractures at depths greater than 80 fbgf. The K zones of the upper and deeper zones assigned to the flow model are shown in Figure 11 (a) and (b). Porosity in unconsolidated formations is derived from the pore spaces within the sediments, while in consolidated rock formations from spaces within fractures, joints, faults, and bedding planes. The overall effective porosity and total porosity assigned to basement rocks are 10 and 20% respectively. The effective and total porosity values assigned to the topsoil layer are 10 and 40% respectively. The porosity values defined in the model are given in Table 3.

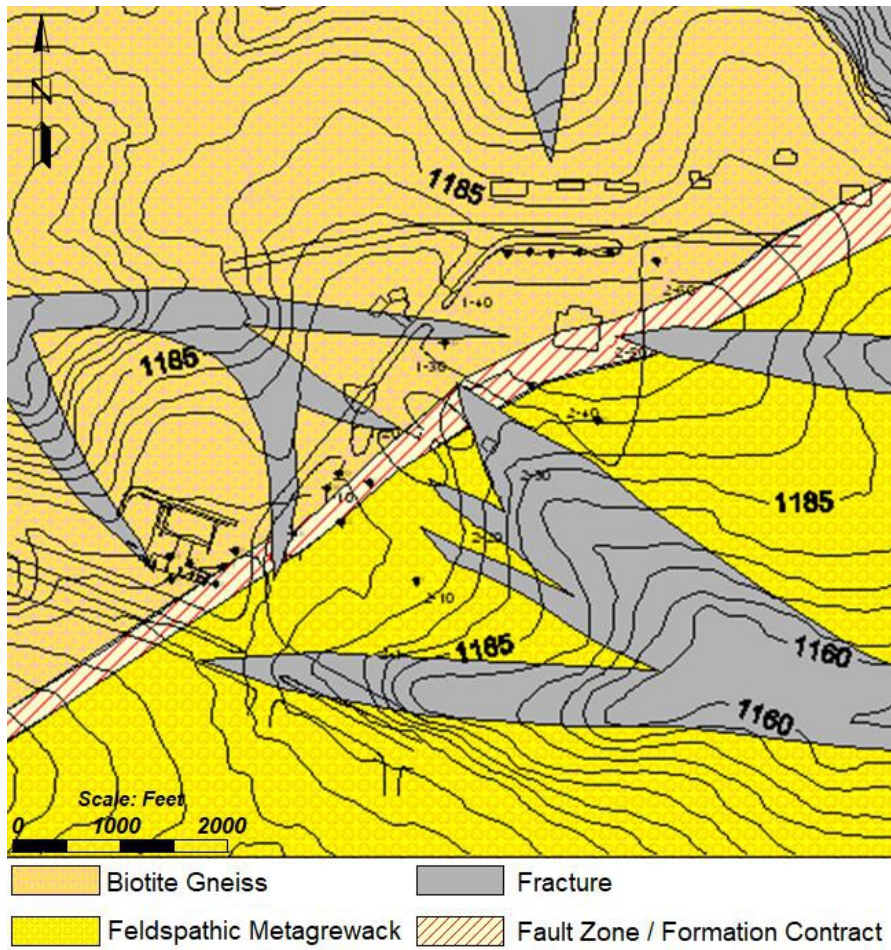


Fig. 9. Conceptual geologic model of study area.

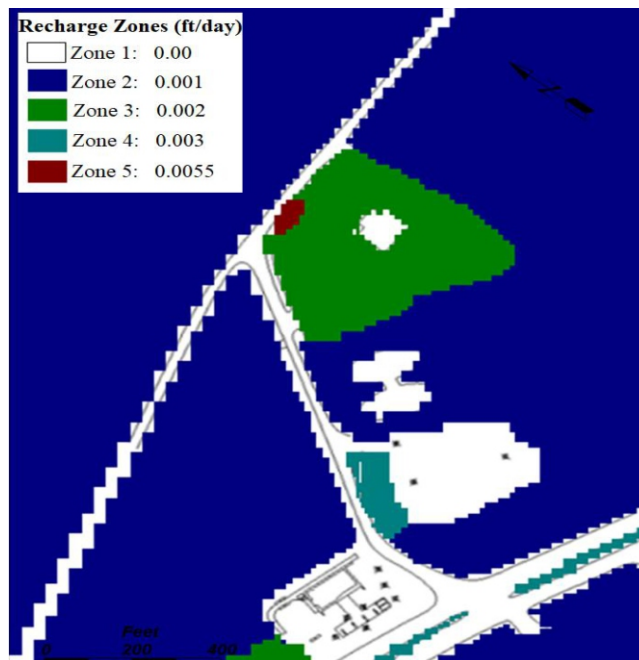


Fig. 10. The recharge zones of site area applied on top layer of the model domain.

There are numerous supply wells in the study area, including the well for the residences along Wirtz Road. These include the subjects of this modeling effort, SW-7, and SW-9. All of these wells withdraw water on a daily basis. These wells are not considered in the model because 1) no construction information is available for the wells on which to base the definition of the

wells, and 2) the lack of pumping offers a more conservative scenario concerning the subsequent transport modeling. The presence of pumping wells in the model would serve to draw water toward the wells and therefore decrease the travel time of groundwater. It also dissolved contaminants from source to the downgradient wells.

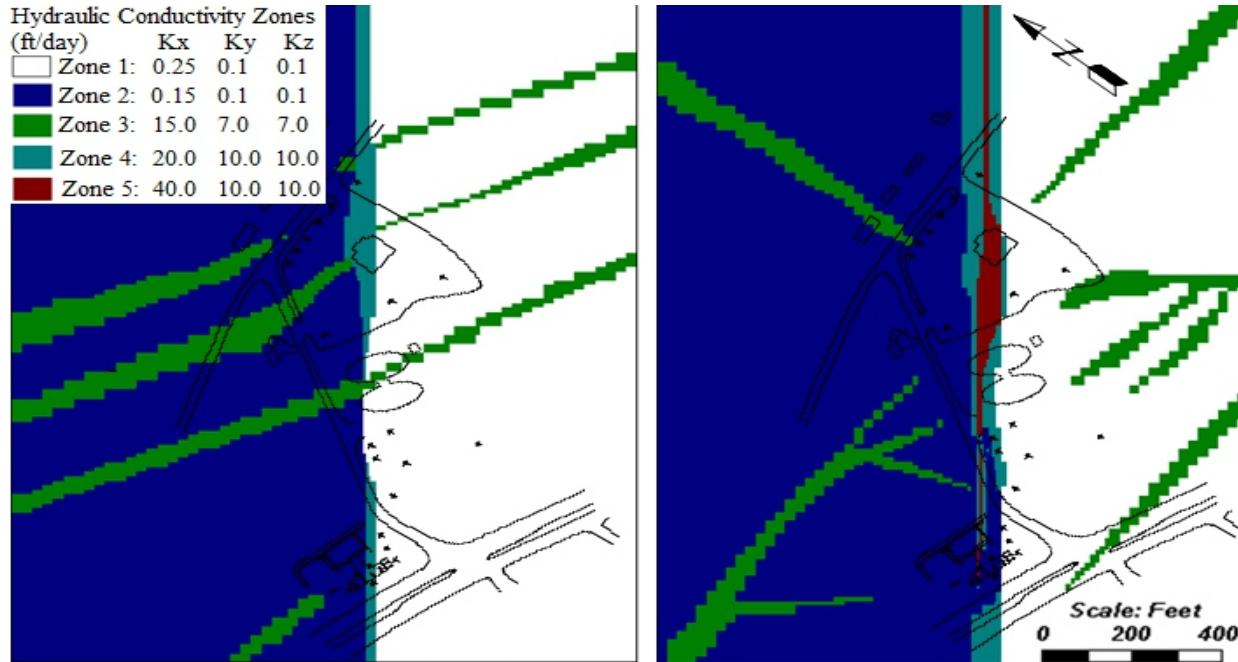


Fig. 11. a). Hydraulic conductivity map of aquifer's upper zone.

Fig. 11. b). Hydraulic conductivity map of aquifer's deeper zone.

Table 2. Slug test analysis results.

Well #	Hydraulic Conductivity (ft/day)	Transmissivity (ft <sup>2</sup> /day)	Calculation Method
MW-4	0.160	1.600	-
MW-6	0.360	3.600	-
MW-9B	0.039	0.387	Bouwer and Rice Graph
	0.040	0.395	Hvorslev Graph
	0.651	6.513	Cooper, Bredehoeft, Papadopoulos
MW-12B	0.538	5.378	-
MW-23	2.615	26.150	Cooper, Bredehoeft, Papadopoulos

Table 3. Flow parameters used in the groundwater flow model.

Parameter	Zone 1	Zone 2	Zone 3	Zone 4	Zone 5	Zone 6
Longitudinal Hydraulic Conductivity $K_x$ (ft/day)	0.25	0.15	15.00	20.00	40.00	0.40
Transverse Hydraulic Conductivity $K_y$ (ft/day)	0.10	0.10	7.00	10.00	10.00	0.10
Vertical Hydraulic Conductivity $K_z$ (ft/day)	0.10	0.10	7.00	10.00	10.00	0.10
Effective Porosity	0.10	0.10	0.10	0.10	0.10	0.10

## 5.2. Flow model calibration

To calibrate the flow model three criteria were defined. The first criterion as an absolute residual mean between the model and target heads of not more than one foot. The second criterion was that no single residual be greater than one foot. The third criterion was that the model flow field has a flow direction and gradient that was consistent with the observed flow field.

The flow model was calibrated by adjusting the boundary conditions, hydraulic conductivity zones, and recharge zones until the calibration criteria were met. The model was calibrated to an absolute residual mean of 0.533 feet, with a residual mean of -0.005 ft. The flow model calibration statistics are presented in Table 4. As per calibration, the absolute residual mean is 3% of the hydraulic head difference over the site. The residuals vs. observed head graph show that the residuals are distributed almost evenly between negative and positive, indicating that there is no significant bias to the residuals (Fig. 12, a). The simulated vs. observed head graph (Fig. 12, b) has a coefficient of determination ( $R^2$ ) between the observed and simulated heads of 0.99, indicating strong agreement. The low absolute residual mean and the high coefficient of determination illustrate the minimal differences between the modeled and observed heads.

The simulated water table map represents the same orientation, direction of flow and hydraulic gradient as that of the average water table map of the area. The minimum and maximum difference between the target heads and model heads are 0.033 feet and -0.949 feet at MW-5 and MW-21, respectively. These data indicate that the overall observed and simulated flow direction and gradient are almost identical. Comparing the contours of the target heads and model heads indicates that the model flow field direction and gradient is representative of the observed flow field direction and gradient. All of the calibration criteria are met by the model. A comparison of the observed and simulated water table maps are shown in Figure 13. The observed and simulated heads along with standard deviation values of the monitoring

data are given in Table 5.

Table 4. Flow model calibration statistics data.

Statistical Parameters	Values (ft)
Minimum Residual	0.033
Maximum Residual	-0.949
Residual Mean	-0.005
Absolute Residual Mean	0.533
Head Range	16.0
Coefficient of Determination ( $R^2$ )	0.99

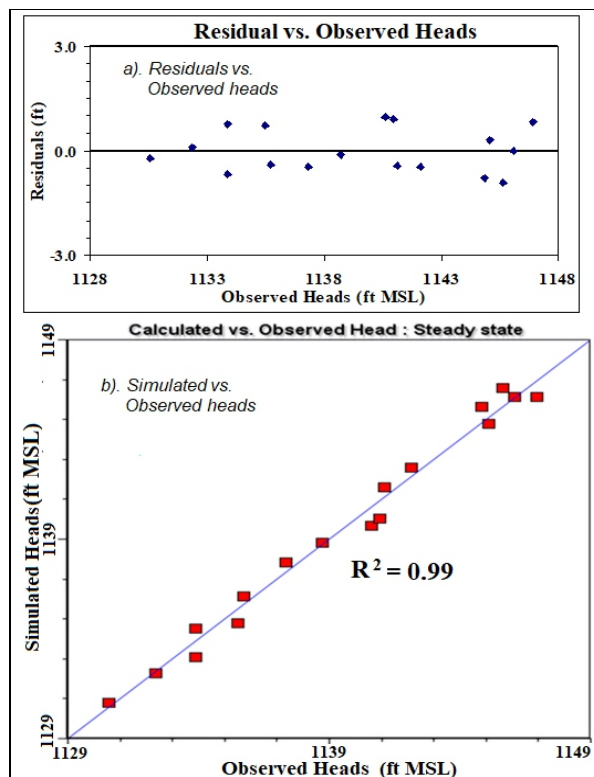


Fig. 12. Statistical Analysis of Flow Model at Seventeen Calibration Targets.

## 6. Transport modeling

Dissolved phase transport modeling was used to determine the impact of the plume on downgradient receptors. The dissolved phase transport model MT3D (Zheng, 1990) was used in the analysis. MT3D uses the flow field from MODFLOW to calculate the transport of solutes in the groundwater with options for considering advection, dispersion, retardation, and chemical reactions of contaminants in groundwater flow systems. Transport simulations were conducted only for Methyl tertiary-Butyl Ether (MTBE) because this is the most mobile of gasoline constituents and the only dissolved constituent observed at the downgradient receptors.

The hydrocarbon was released on October 13, 1999. The previous studies suggest that the source of the release was limited to the immediate vicinity of dispenser No. 3. Residual phase hydrocarbons were observed in soil samples collected during the geoprobe investigation conducted by IMS Environmental Services in 1999, where only one geoprobe location detected BTEX or TPH (Fig. 14). This consists of a limited release, estimated by IMS Environmental Services (2000) to be between 6,500-7,500 liters. The source area in the transport model was defined as 900 ft<sup>2</sup> beneath the dispenser island.

Retardation and decay represent the reduction rate at which dissolved contaminants move through an aquifer due to the sorption of contaminants to the solid aquifer materials. The MTBE does not adsorb well onto aquifer materials and therefore dissolved MTBE tends to move unretarded in the aquifer at the velocity of the groundwater (Squillace, et al., 1998). Field observations suggest that MTBE is not prone to decay (Landmeyer et al., 1998). In light of these facts, the retardation and decay factors for MTBE were not considered in this study.

The  $K_x$  is usually greater than  $K_y$ , this is obvious in anisotropic conditions as imposed at site's foliated metamorphic rocks. This is evidenced in the observed plume by its narrow lateral extents. As a first approximation, the  $K_x$  can be defined as 10 percent of the plume flow path (Fetter, 1988). This would mean  $K_x$  of more than 100 ft. A dispersivity value of that magnitude would result in extremely rapid downgradient plume migration. In order to maintain a conservative approach to the modeling of the dissolved transport, the  $K_x$  was conservatively defined as 10 ft. To reflect the strong anisotropy in the aquifer, the transverse dispersivity was defined as 1% of the longitudinal dispersivity.

### 6.1. Transport model calibration

Calibration was achieved by defining the source concentration as approximately 70% of the solubility of MTBE. Peters, et al., (2002) described the temperature-dependent solubility of MTBE to be approximately 42,000 ppb at

55oF, the assumed aquifer temperature. Using the transport parameters a source concentration of 30,000 ppb (30 mg/l) was assigned to the model. Three criteria were defined for the transport model calibration. First, the maximum residual between observed and simulated concentration should be less than 1 mg/l. The second criterion was defined that the absolute residual mean between the model and target concentrations should be less than 10% of the total concentration difference over the site for the most recent monitoring event of April 4, 2007. For this event concentrations ranged from 0.01 mg/l at MW-3 to 19.0 mg/l at MW-11 with a difference of 18.99 mg/l.

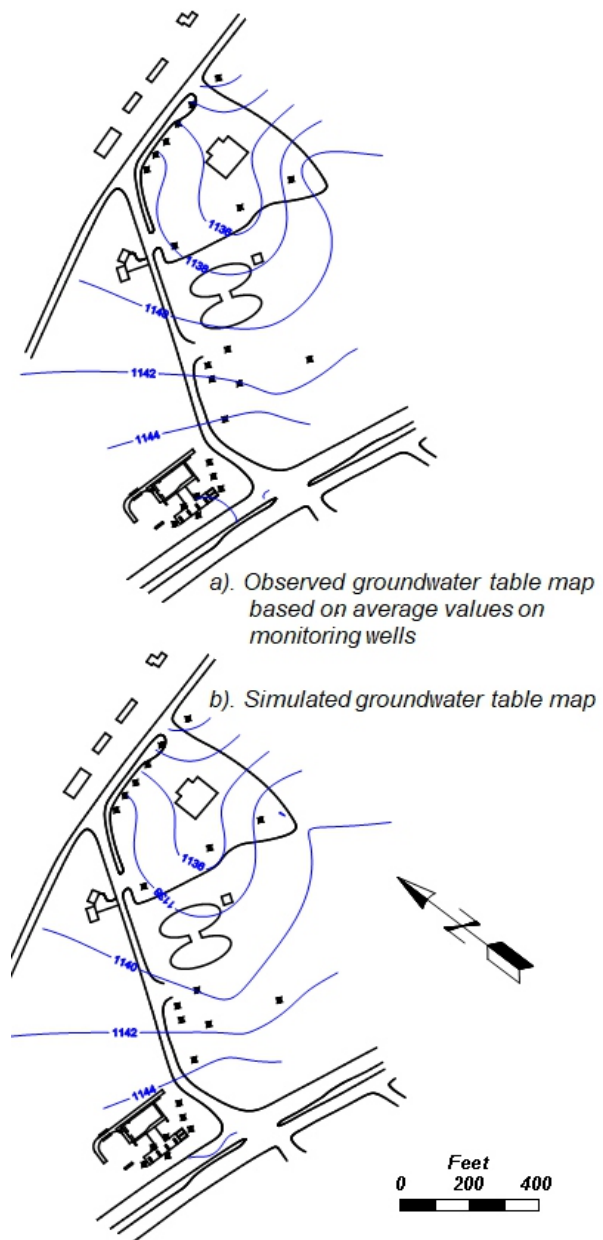


Fig. 13. Groundwater table contours based on observed and simulated values.

The second calibration criterion was defined as an absolute residual mean of 1.9 mg/l or less. The third calibration criterion was that 65% or more of the analytical results for a comprehensive sampling event in each year should follow the first two criteria. Sampling events from 12/12/03, 8/18/04, 6/30/05, 6/29/06, and 4/4/07 were selected for calibration analysis because these events contained a large number of samples to judge the transport calibration. The most comprehensive event was 4/4/07 which consisted of samples from 19 of the 26 wells. The calibration statistics for wells meeting the

first two criteria for the most comprehensive and recent sampling event of 4/4/07 is given in Table 6. All of the other representative sampling events for each year also met the three criteria. The observed and simulated concentrations for those targets of 12/12/03, 8/18/04, 6/30/05, 6/29/06, and 4/4/07 that meet the first two criteria, along with the minimum and maximum simulated residuals are presented in Table 7. The transport calibration of residual vs. observed MTBE of 4/4/07 is illustrated graphically in Figure 15. The graph illustrates a strong coefficient of correlation of 0.99, with no significant bias to the residuals.

Table 5. Flow model calibration results data.

Well #	Observed Heads (ft)	Simulated Heads (ft)	Standard Deviation (ft)
MW-1	1144.85	1145.62	0.77
MW-2	1145.64	1146.56	0.92
MW-3	1146.95	1146.12	-0.83
MW-5	1146.11	1146.14	0.03
MW-7	1142.12	1142.58	0.46
MW-8	1140.94	1140.04	-0.9
MW-9	1135.72	1136.13	0.41
MW-9B	1133.90	1134.53	0.63
MW-10	1137.35	1137.83	0.48
MW-11	1130.58	1130.79	0.21
MW-12	1132.37	1132.29	-0.08
MW-12B	1133.90	1133.09	-0.81
MW-13	1135.48	1134.78	-0.70
MW-16	1138.73	1138.84	0.11
MW-18	1145.09	1144.79	-0.30
MW-21	1140.61	1139.66	-0.95
MW-22	1141.13	1141.58	0.45

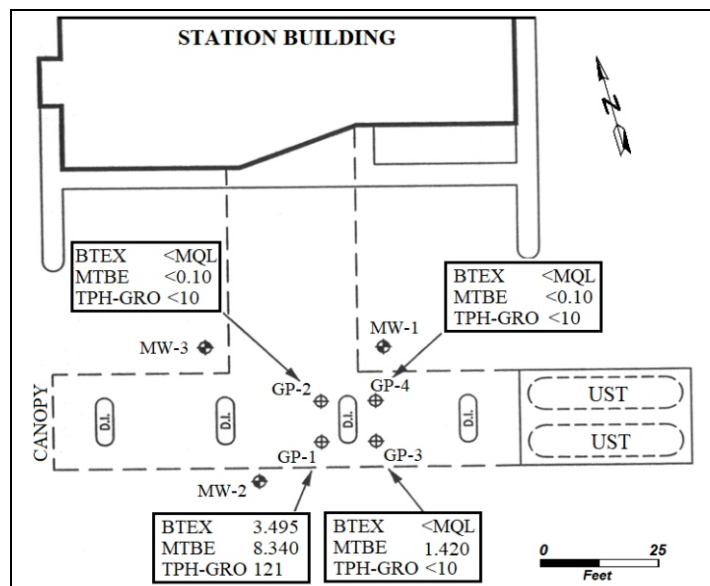


Fig. 14. Location sketch of observed residual phase hydrocarbons, (IMS, 2000).

## 6.2. Transport time to receptors

The model aquifer is divided into an upper and a deeper zone on the basis of the geologic and hydrogeologic data. The groundwater movement is faster in the lower zone as compared to the upper zone of the aquifer, due to higher K at deeper fracture zones. The transport times of the MTBE plume in the upper and lower zones of the aquifer with reference to specific locations, estimated days and corresponding dates calculated. In the deeper zone of the aquifer, the model plume enters the property area of well No. MS-7 810 days at December 31, 2001, as compared to 865 days in the upper zone of the aquifer on February 24, 2002, (Fig. 16). The simulated MTBE plume entered the property area of well No. MS-9 in 1064 days on September 11, 2002, in the deeper zone of the aquifer, while in 1096 days on October 13, 2002, in the upper zone of the aquifer, (Fig. 17).

Groundwater analysis of dissolved MTBE at the first receptor water supply well No. SW-7 was conducted three times on September 1, 2003, November 3, 2003, and July 13, 2006. The observed concentration varies from 0.01 to 0.012 mg/l. The second receptor water supply well No. SW-9 was sampled on December 10, 2003, April 22, 2004, and lastly on July 3, 2006. The observed concentrations were 0.042, 0.038 and 0.003 mg/l respectively. The SW-7 and SW-9 are located at the northern edge of the contaminant plume. The simulated concentrations at SW-7 are consistent with the observed concentrations, but the model underpredicts the concentrations at SW-9 (Table 8). SW-9 is located such that the simulated plume remains far enough to south that concentrations do not appear at the well. The most likely explanation for this is that SW-9 is connected to fractures that intercept the dissolved plume. This is not accounted for in the model because there is a paucity of data in that region of the model domain on which to base the connection. Moreover, the pumping from SW-9 is not simulated, which would serve to draw contaminants toward it. The change in concentration overtime at the wells property boundaries was evaluated in intervals of 1.0, 2.5, 5.0, 7.5, 10.0, and 25  $\mu\text{g/l}$ , results are presented in Table 9.

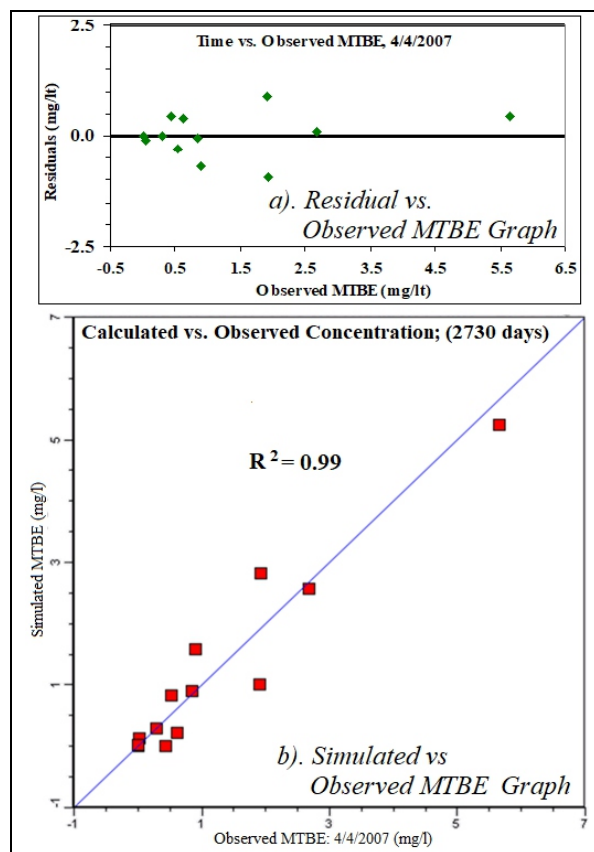


Fig. 15. Statistical Analysis of the transport model calibration, MTBE mg/l as on 4/4/07 analysis.

Table 6. Transport model calibration statistics for the 4/4/07 sampling event.

Statistical Parameter	Values
Minimum Residual	-0.003 (mg/l)
Maximum Residual	0.908 (mg/l)
Absolute Residual Mean	0.35 (mg/l)
Concentration Range	18.99 mg/l
Coefficient of Determination ( $R^2$ )	0.996

## 7. Sensitivity analysis

The principal parameters affecting the speed of plume migration are K, dispersivity, and source concentration. For many dissolved contaminants, retardation is an important parameter but because MTBE is known to move unretarded in groundwater systems, retardation was not considered in this analysis. The sensitivity analysis evaluated the response to the model by incremental increases and decreases in K, dispersivity, and source concentration. Six K zones (Z) are employed in flow modeling. The flow model response was observed with a 10% to 15% increase and a decrease in K values. The flow model was run

Table 7. Summary of MTBE calibration results over time (mg/l).

Well #	12/12/2003		8/18/2004		6/30/2005		6/29/2006		4/4/2007	
	Observed	Simulated	Observed	Simulated	Observed	Simulated	Observed	Simulated	Observed	Simulated
MW-2	-	-	0.26	0.13	0.29	0.16	0.25	0.19	0.61	0.21
MW-3	-	-	0.01	0.02	0.01	0.04	0.00	0.05	-	-
MW-4	-	-	0.01	0.00	0.01	0.00	0.00	0.00	-	-
MW-5	-	-	-	-	-	-	-	-	1.92	2.83
MW-7	0.01	0.00	0.01	0.00	0.01	0.00	0.00	0.00	-	-
MW-8	0.01	0.00	0.01	0.00	0.01	0.00	0.00	0.00	-	-
MW-9	0.04	0.00	0.09	0.01	0.08	0.01	-	-	0.01	0.02
MW-9B	-	-	-	-	-	-	-	-	0.90	1.59
MW-10	0.01	0.00	-	-	0.01	0.00	0.00	0.00	-	-
MW-11	0.10	0.16	0.01	0.30	0.05	0.50	0.05	0.70	0.53	0.83
MW-12	0.01	0.01	0.01	0.03	0.02	0.06	0.05	0.10	0.03	0.12
MW-12B	-	-	-	-	-	-	0.07	0.02	0.01	0.02
MW-13	0.01	0.00	0.04	0.00	0.08	0.00	0.09	0.00	0.43	0.00
MW-14	0.01	0.00	-	-	0.01	0.00	-	-	0.01	0.00
MW-15	0.01	0.00	-	-	0.01	0.00	0.00	0.00	-	-
MW-16	0.01	0.00	-	-	0.01	0.00	-	-	-	-
MW-17	-	-	-	-	-	-	-	-	19.00	19.89
MW-18	-	-	-	-	-	-	-	-	-	-
MW-19	-	-	-	-	-	-	-	-	5.65	5.23
MW-20	-	-	0.52	1.05	-	-	-	-	2.67	2.57
MW-21	-	-	0.04	0.04	0.04	0.09	0.05	0.19	0.30	0.30
MW-21B	-	-	-	-	-	-	-	-	1.91	1.02
MW-22	-	-	0.07	0.17	0.07	0.36	0.11	0.65	0.84	0.91
Min R*	-	-0.005	-	0.00	-	-0.005	-	0.00	-	-0.003
Max R*	-	0.061	-	0.53	-	0.445	-	0.655	-	0.908
Targets	-	77%	-	67%	-	68%	-	65%	-	79%

\*Min R = Minimum Residual, Max R = Maximum Residual



Fig. 16. a) The simulated MTBE plume in deeper zone of the aquifer entered the property area of MS-7 in 810 days. b) In upper zone, the plume enters after 865 days.

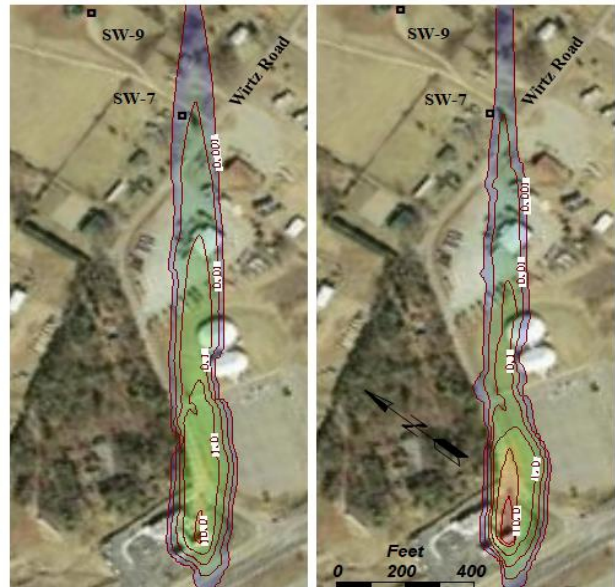


Fig. 17. a) The simulated MTBE plume in deeper zone of the aquifer entered the property area of MS-9 in 1064 days. b) In upper zone, the plume enters after 1096 days.

Table 8. Observed and simulated MTBE concentrations at the receptor wells.

Observed/Simulated	MTBE (mg/l)	Days after Release	Corresponding Dates
<b>Property of Well No. SW-7</b>			
<b>Simulated</b>	0.00	810	December 31, 2001
	0.00	1000	July 9, 2002
	0.001	1222	February 16, 2003
<b>Observed</b>	0.01	1419	September 1, 2003
	0.011	1482	November 3, 2003
<b>Simulated</b>	0.017	1642	April 11, 2004
<b>Property of Well No. SW-9</b>			
<b>Simulated</b>	0.00	1064	September 11, 2002
	0.00	1222	February 16, 2003
	0.00	1405	August 18, 2003
<b>Observed</b>	0.042	1519	December 10, 2003
	0.038	1653	April 22, 2004
<b>Simulated</b>	0.00	1952	February 15, 2005
	0.00	2172	September 23, 2005
<b>Observed</b>	0.003	2455	July 3, 2006

Table 9. Simulated concentration over time at the property boundaries.

Contour Concentration		Property of SW-7		Property of SW-9	
µg/l	mg/l	Days after release	Corresponding Dates	Days after release	Corresponding Dates
<b>1.0</b>	<b>0.001</b>	810	December 31, 2001	1064	September 11, 2002
<b>2.5</b>	<b>0.0025</b>	870	March 2, 2002	1200	January 25, 2003
<b>5.0</b>	<b>0.005</b>	912	April 12, 2002	1250	March 16, 2003
<b>7.5</b>	<b>0.0075</b>	942	May 31, 2002	1300	May 5, 2003
<b>10.0</b>	<b>0.01</b>	972	June 11, 2002	1350	June 24, 2003
<b>25.0</b>	<b>0.025</b>	1064	September 11, 2002	1450	October 2, 2003

with a systematic increase and decrease of K values together first in zones 1 and 2, then zones 1, 2, and 3, then zones 4 and 5, and lastly in all zones. Of particular importance is the response to zones 4 and 5 which have the highest conductivities and through which most of the contaminant transport is taking place. The base values of K and 10% to 15% increased and decreased values used in the flow model and in sensitivity analysis are presented in Table 10. The minimum and maximum residuals of the calibrated flow model are less than one and vary from 0.003 to -0.949 ft respectively. With the change of K values in some and all zones, the values of maximum residuals increased to more than one in almost all scenarios (Table 11). One of the flow model calibration criteria is to maintain the minimum and maximum target head residual less than one. Moreover, most of the scenarios also result in an increase in the absolute residual mean. The increase and a decrease in K value considerably affect the flow model, which reveals that the flow model is

very sensitive to changes in K. Analysis reveals that any changes in conductivity are detrimental to the flow calibration.

To observe the sensitivity of the contaminant transport model to dispersion in the aquifer material, a sensitivity analysis was conducted with variations on the longitudinal and lateral dispersivity values. The base value of longitudinal dispersivity was 10 ft, while the vertical and horizontal dispersivities were defined as 0.1 ft. These values were increased by 10%, 20% and 50% to observe the sensitivity of the model. The base dispersivity values and proportionally increased and decreased dispersion values used in the sensitivity analysis are represented in Table 12. The calibrated minimum and maximum target concentration values of the transport model with base values vary from -0.003 to 0.908 mg/l. By utilizing the incremental decreases in dispersivity values, the maximum residuals between target concentrations and model

concentrations increased considerably in each case (Table 13) and vary from 1.06 to 2.947 mg/l. The increases in dispersivity resulted in an increase in the maximum residuals of between 1.848 mg/l and 5.987 mg/l. All of these maximum residuals are above that defined for the transport model calibration criterion. Not only did these changes result in an increase in maximum residual to above the calibration criterion, but with only one exception did the absolute residual mean increase. These data indicate that the transport model is highly sensitive to the dispersivity and that any change to these values is detrimental to the calibration.

Sensitivity analysis of source concentration was conducted with 10%, 15% and 20% increase and decrease in the source concentration. The calibrated transport model

used a source concentration of 30,000 ppb (30 mg/l) and resulted in a minimum residual of 0.003 mg/l and a maximum residual of 0.908 mg/l. The incremental decreases in source concentration resulted in maximum residuals ranging from -1.700 to -1.806 mg/l (Table 14). The incremental increases in source concentration resulted in maximum residuals ranging from 5.141 to 7.336 mg/l. All of these maximum residuals are above that defined for the transport model calibration criterion. Not only did these changes result in an increase in maximum residual to above the calibration criterion, but in every case, the absolute residual mean increased. These data indicate that the transport model is highly sensitive to the source concentration and that any change to the source concentration is detrimental to the calibration.

Table 10. Hydraulic conductivity values used in sensitivity analysis (ft/day).

H. C. Zones	Base Values			10% Increase			10% Decrease			15% Increase			15% Decrease		
	K <sub>x</sub>	K <sub>y</sub>	K <sub>z</sub>	K <sub>x</sub>	K <sub>y</sub>	K <sub>z</sub>	K <sub>x</sub>	K <sub>y</sub>	K <sub>z</sub>	K <sub>x</sub>	K <sub>y</sub>	K <sub>z</sub>	K <sub>x</sub>	K <sub>y</sub>	K <sub>z</sub>
Z-1	0.25	0.10	0.10	0.28	0.10	0.10	0.23	0.10	0.10	0.2875	0.10	0.10	0.2125	0.10	0.10
Z-2	0.15	0.10	0.10	0.17	0.10	0.10	0.14	0.10	0.10	0.1725	0.10	0.10	0.1275	0.10	0.10
Z-3	15.00	7.00	7.00	16.50	8.00	8.00	13.50	7.00	7.00	17.25	8.00	8.00	12.75	6.00	6.00
Z-4	20.00	10.00	10.00	22.00	11.00	11.00	18.00	9.00	9.00	23.00	11.00	11.00	17.00	8.00	8.00
Z-5	40.00	10.00	10.00	44.00	11.00	11.00	38.00	10.00	10.00	46.00	12.00	12.00	34.00	10.00	10.00
Z-6	0.40	0.10	0.10	0.44	0.10	0.10	0.36	0.10	0.10	0.46	0.10	0.10	0.34	0.10	0.10

Table 11. Simulated minimum and maximum residual heads with change of hydraulic conductivity values in sensitivity analysis (ft).

Hydraulic C. Zones	Calibrated Values		10% Increase		10% Decrease		15% Increase		15% Decrease	
	Max R	ARM	Max R	ARM	Max R	ARM	Max R	ARM	Max R	ARM
Z-1, 2	-0.949	0.533	-1.018	0.559	-1.155	0.521	-1.072	0.566	-1.258	0.515
Z-1, 2, 3	-0.949	0.533	-0.959	0.57	-1.248	0.518	1.044	0.582	-1.417	0.523
Z-4, 5	-0.949	0.533	-1.46	0.534	1.142	0.613	-1.697	0.623	1.539	0.681
Z-1, 2, 3, 4, 5, 6	-0.949	0.533	-1.165	0.541	0.957	0.579	-1.261	0.55	1.087	0.622

Table 12. Dispersivity data used in sensitivity analysis.

Dispersivity (ft)	Base Values	10%		20%		50%	
		Increase	Decrease	Increase	Decrease	Increase	Decrease
Longitudinal	10.0	11.0	9.0	12.0	8.0	15.0	5.0
Horiz./Long.	0.1	0.11	0.09	0.12	0.08	0.15	0.05
Vert./Long.	0.1	0.11	0.09	0.12	0.08	0.15	0.05

Table 13. Simulated minimum and maximum residual concentrations by use of different dispersivity values in sensitivity analysis.

Residuals (mg/l)	Base Values	10%		20%		50%	
		Increase	Decrease	Increase	Decrease	Increase	Decrease
Minimum	-0.003	-0.005	-0.005	-0.005	-0.005	-0.004	-0.003
Maximum	0.908	1.848	1.06	2.854	1.32	5.987	2.947
ARM*	0.35	0.403	0.331	0.476	0.416	0.725	0.663

\*ARM=absolute residual mean.

Table 14. Simulated minimum and maximum residual concentrations by use of different source concentration values in sensitivity analysis.

	Base	10%		15%		20%	
	Values	Increase	Decrease	Increase	Decrease	Increase	Decrease
<b>MTBE (mg/l)</b>	30.0	33.0	27.0	34.5	25.5	36.0	24.0
<b>Minimum Residual</b>	-0.003	-0.005	-0.005	-0.005	-0.005	-0.005	-0.005
<b>Maximum Residual</b>	0.908	2.881	-1.098	3.875	-2.092	4.87	-3.087
<b>ARM*</b>	0.35	0.502	0.387	0.613	0.47	0.723	0.552

\*ARM=absolute residual mean.

## 8. Conclusion

The modeling effort was conducted with a considerable amount of geologic, hydrogeologic, and dissolved concentration data spanning over approximately eight years. The resulting model is sophisticated and calibrated to a high standard, both for flow and for transport. Based on the modeling results it has been concluded that the dissolved MTBE crossed the property boundary of well No. MS-7 in the deep zone on December 31, 2001, and entered the property area of MS-9 on September 11, 2002.

Based on the model, this is likely to represent the slowest movement onto those properties because pumping from the supply wells were not considered in the flow model. This is conservative in that simulating pumping from those wells would draw water and dissolved contaminants to the wells and speed up the plume migration. The dispersivity in the transport model was conservatively defined at 10 feet. This is conservative because the first approximation in defining dispersivity in models is usually considered to be 10% of the plume length. In this case, the dispersivity value of more than 100 ft would result in faster plume migration in simulation. The sensitivity analysis revealed that the model is highly sensitive to changes in any of the parameters that would affect the speed of the plume. Any changes to those parameters, including changes that would slow the migration of the simulated plume, were detrimental to the calibration of the model.

## Acknowledgment

The abstract of the study was presented and highly acknowledged in the “Baki Canik Water Civilization Symposium” held on

October 7-9, 2013 Aksaray University, Turkey.

## Author’s Contribution

*Syed Mobasher Aftab prepared and improved conceptual geological model of the study area that served as a base for the mathematical groundwater modeling. With the help of eight years collected data-sets Syed conducted groundwater flow and transport modeling of MTBE. He calibrated the flow model, conducted sensitivity analysis, and the time of travel of contaminated plume was simulated up to the property boundaries of the impacted water supply wells.*

*Warren T Dean proposed the main perception of groundwater modeling and finalized the major portion of the paper write-up. Groundwater inventory, monitoring, piezometer drilling, and pump test analysis were conducted under the direct supervision of Warren. The groundwater sampling, chemical analysis and interpretations were conducted under his observations and guidance. He was also liable for the technical quality of the research and to present the progress at different stages and levels.*

## References

- Apex Environmental, Inc., 2003. Post site characterization monitoring, stopin-plateau plaza, 20430 Virgil H. Goode highway, Rocky Mount, apex environmental, Inc., Roanoke, Virginia.
- ATS International., 2004. Hydrogeologic analysis and groundwater flow and transport modeling for the stopin-plateau plaza site. 20430 Virgil H. Goode highway, Rocky Mount, Virginia 24151. PC 00-2043, Facility ID 2-021672. ATS International, Inc. 107 Lester St. Christiansburg, Virginia.

- Crawford Environmental Services., 2003. Site Characterization Report Addendum No. 2, StopIn-Plateau Plaza, 20430 Virgil H. Goode Highway, Rocky Mount, VA 24141, FAC. ID #2-021672, PC #00-2043, Crawford Environmental Services, Inc., Daleville, Virginia.
- Crawford Environmental Services, 2004a. Site Characterization Report Addendum No. 3, StopIn-Plateau Plaza, 20430 Virgil H. Goode Highway, Rocky Mount, VA 24141, FAC. ID #2-021672, PC #00-2043, Crawford Environmental Services, Inc., Daleville, Virginia.
- Crawford Environmental Services, 2004b. Site Characterization Report Addendum No. 4, StopIn-Plateau Plaza, 20430 Virgil H. Goode Highway, Rocky Mount, VA 24141, FAC. ID #2-021672, PC #00-2043, Crawford Environmental Services, Inc., Daleville, Virginia.
- Crawford Environmental Services, 2004c. Site Characterization Report Addendum No. 5, StopIn-Plateau Plaza, 20430 Virgil H. Goode Highway, Rocky Mount, VA 24141, FAC. ID #2-021672, PC #00-2043, Crawford Environmental Services, Inc., Daleville, Virginia.
- ECS Mid-Atlantic, LLC, 2005. Characterization Report Addendum No. 6, StopIn-Plateau Plaza, 20430 Virgil H. Goode Highway, Rocky Mount, VA 24141, FAC. ID #2-021672, PC #00-2043. ECS Mid-Atlantic, LLC, 5320 Peters Creek Road, Suite F, Roanoke, VA 24019.
- ECS Mid-Atlantic, LLC, 2006a. Characterization Report Addendum No. 7, StopIn-Plateau Plaza, 20430 Virgil H. Goode Highway, Rocky Mount, VA 24141, FAC. ID #2-021672, PC #00-2043. ECS Mid-Atlantic, LLC, 5320 Peters Creek Road, Suite F, Roanoke, VA 24019.
- ECS Mid-Atlantic, LLC, 2006b. Characterization Report Addendum No. 8, StopIn-Plateau Plaza, 20430 Virgil H. Goode Highway, Rocky Mount, VA 24141, FAC. ID #2-021672, PC #00-2043. ECS Mid-Atlantic, LLC, 5320 Peters Creek Road, Suite F, Roanoke, VA 24019.
- ECS Mid-Atlantic, LLC, 2007. Corrective Action Plan Plateau Plaza Exxon, Rocky Mount, Virginia. ECS Mid-Atlantic, LLC, 5320 Peters Creek Road, Suite F, Roanoke, VA 24019.
- Fetter, C. W., 1988. Applied Hydrogeology, Merrill Publishing Company, Columbus, Ohio, 591.
- Fleck, W. R., White, R. K., 1989. Effects of remnant foliation on the hydrologic properties of piedmont saprolite: in ground water in the Piedmont. In: Daniel, C.C., White, R. K., Stone, P. A., (Eds.), Proceedings of a Conference on Ground Water in the Piedmont of the Eastern United States, Clemson University, Clemson, South Carolina, 693.
- Harned, D. A., Daniel, C.C., 1989. The transition zone between bedrock and regolith: conduit for contamination? in ground water in the Piedmont. In: Daniel, C. C, White, R. K. Stone, P. A. (Eds.), Proceedings of a Conference on Ground water in the Piedmont of the Eastern United States, Clemson University, Clemson, South Carolina, 693.
- Henika, W. S., 2004. Written and oral communication, Christiansburg, Virginia.
- IMS Environmental Services, 2000. Site Characterization Report, Plateau Plaza, Route 220, Franklin County, Virginia, IMS Environmental Services, Morgantown, West Virginia.
- Landmeyer, J. E., Chapelle, F. H., Bradley, P. M., Pankow, J. F., Church, C. D., Trattnyek, P. G., 1998. Fate of MTBE relative to benzene in a gasoline contaminated aquifer. Ground Water Monitoring & Remediation, Fall 1998, 93-102.
- McDonald, M. G., Harbaugh, A. W., 1988. A modular three-dimensional finite-difference ground-water flow model, Department of the Interior, U.S. Geological Survey.
- Peters, U., Nierlich, F., Sakuth, M., Laugier, M., 2002. Methyl tert-butyl ether, physical and chemical properties, Ullmanns Encyclopedia of industrial chemistry, Release 2003, 6th ed., VCH Verlag GmbH & Co. KGaA, Wiley, DOI, 10.1002/14356007.a16\_543.
- Squillace, P. J., Pankow, J. F., Korte, N. E.,

Zogorski, J. S., 1998. Environmental behavior and fate of methyl tert-butyl ether (MTBE). USGS Fact Sheet FS-203-96

Waterloo Hydrogeologic Inc., 2006. Visual MODFLOW v.4.2 for professional applications in three-dimensional groundwater flow and contaminant transport modeling. Waterloo Hydrogeologic, Inc. A Schlumberger Company, 460 Phillip St. Suite 101, Waterloo, ON. Canada N2L 5J2.

Zheng, C., 1990. MT3D, a modular three-dimensional transport model, S.S. Papadopoulos & Assoc., Rockville, MD.